A Novel Multi-Scale Numerical Model for Prediction of Texture-Related Impacts on Fuel Consumption

Dmytro A. Mansura*
mansura@uni-wuppertal.de
Pavement Research Centre
Department of Civil Engineering, Faculty D
University of Wuppertal
Pauluskirchstraße, 7
Wuppertal, North-Rhein Westfalia, 42285
Germany

Nicholas H. Thom
nicholas.thom@nottingham.ac.uk
Nottingham Transportation Engineering Centre
Department of Civil Engineering
Faculty of Engineering
University of Nottingham
University Park
Nottingham, Nottinghamshire, NG7 2RD
United Kingdom

Hartmut J. Beckedahl
beckedahl@uni-wuppertal.de
Pavement Research Centre
Department of Civil Engineering, Faculty D
University of Wuppertal
Pauluskirchstraße, 7
Wuppertal, North-Rhein Westfalia, 42285
Germany

Presented at the thirty fourth annual meeting
of The Tire Society, Akron, Ohio,
September 8–9, 2015.

*Presenter/Corresponding author.

REFERENCE: Mansura, D. A., Thom, N. H. and Beckedahl, H.J., "**A Novel Multi-Scale Numerical Model for Prediction of Texture-Related Impacts on Fuel Consumption**," submitted for presentation at the 2015 Tire Society meeting, and for consideration for publication in the journal *Tire Science and Technology*.

ABSTRACT: It is estimated that to overcome rolling resistance (RR) a typical vehicle on average consumes 4152 MJ/119 litres of fuel annually depending not only on vehicle-related factors but also pavement-related ones. A slight improvement in surface properties may thus decrease fuel consumption bringing substantial long-term socio-economic benefits per capita/country. This aligns with ever-tighter limits on CO_2 in the EU (95 g/km until 2021) fostering sustainable construction/exploitation of tyres and pavements. This paper outlines a newly developed multi-scale 3-D numerical methodology to quantify texture-dependent RR due to indentation of aggregates into visco-elastic tread compound. It consists of a micro-scale tread block - single aggregate model and a macro-scale car tyre finite element model, rolling in a steady state mode over a rigid smooth surface. Micro-scale interaction rates are deduced from the macro-scale model. Tread compound is simulated by application of a time-dependent linear visco-elastic model. The micro-scale simulations enabled quantification of RR induced by an arrangement of surface aggregates. The outlined texture-dependent RR estimates are based on contact force moment around the contact patch centre. The computed contact force results show a significant peak of normal force due to visco-elastic and inertia effects at the onset of the tyre-surface contact phase, followed by a gradually decreasing/relaxing stress region with a sudden release at the end of the interaction. The contact forces appear to be of a reasonable distribution and magnitude. The proposed approach allows prediction of RR losses due to compressive forces at the micro-scale. Macro-distortional RR (which is not the subject of this paper) would then have to be added to find the total tyre-related RR.

KEY WORDS: rolling resistance, tread block, hemispherical aggregate, multi-scale model, vertical velocity, contact mechanics, fuel consumption

Introduction

In view of an escalating transportation demand, particularly in the USA and Europe, ever-stricter regulatory emission limits (95 g/km by 2021 in the EU) are being enforced by governments all over the world to minimize detrimental impact on the quality of life. Both vehicle/tyre and pavement research centers are therefore in constant search of ways to enable operation of tyres and roadways at an increased sustainability level. While vehicle and tyre makers, and now also highway institutes, have made considerable progress in enhancing fuel economy in terms of aerodynamic drag, drive-train and tyre/roadway rolling resistance (RR) [1, 2], pavements represent a potential key to further reducing energy loss. It is estimated that to overcome RR a typical vehicle on average consumes 4152 MJ/119 litres of fuel yearly depending not only on *tyre*-related characteristics such as structural composition or material compound properties, but also on *pavement*-related factors, of which weak pavement structure and rough texture have been found to cause extra fuel consumption [3, 4].

RR is a cumulative term that comprises a suite of energy loss mechanisms, whose total value typically ranges from 25 to 80 N per car tyre [19]. These energy losses vary in magnitude and simultaneously occur because of the following causes:

- tyre macro-distortional, mainly visco-elastic dissipation (texture-independent)
- micro-distortional visco-elastic and inertial dissipation (texture-dependent)
- pavement macro-distortional dissipation (texture-independent)

Texture-independent energy dissipation in the tyre is generally attributed to macro-distortional hysteresis that appears as a result of compressive, tangential (shearing/micro-slippage and shear-related inertia) and wave-induced inertial deformations. The deformation is caused by flattening of the contacting tread part leading to compression, shearing and bending of the tread part and bending of the crown, sidewall and bead elements. Shear-induced inertial forces are activated when the tread is in a slippage phase and are usually

incorporated into a resultant tangential force. According to Michelin [5], tread compression and longitudinal shearing share the greatest portion of the energy consumption. Additionally, the losses could be amplified by standing waves, centrifugal and to lesser extent Corriolis forces.

Micro-distortional losses are triggered by aggregate indentations into elastomeric tread compound. These indentations generate local compression which includes a visco – elastic and an inertial component that affect the moment balance in the contact region. Figure 1 illustrates that this part of RR is dependent on penetration of individual stones and the distance between adjacent asperities.

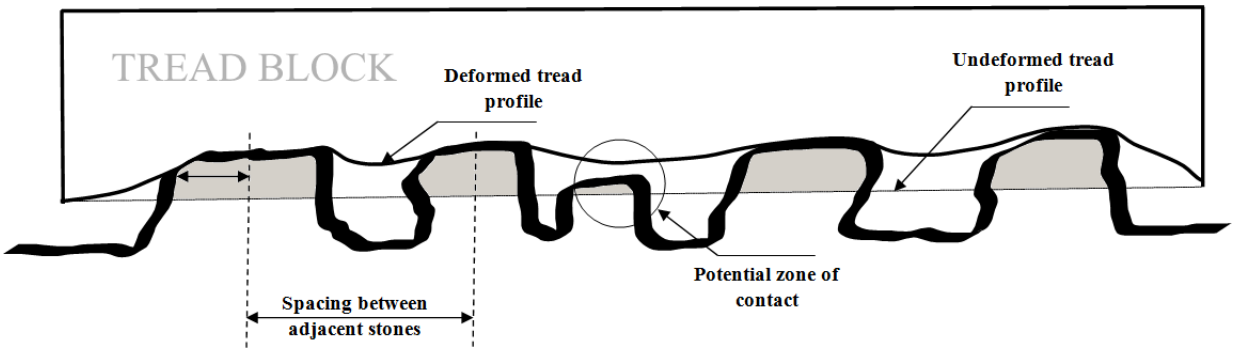

Figure 1 Close-up view of multi-indentation effects as a result of array of stones (not to scale)

The presence of road protrusions could slightly modify tread-related tangential stresses/excitations, which were included in the macro-distortional term, permitting the tread block to rise and descend throughout the stick-slip phase. Aggregate texture, tread block shape and in general tyre profile all influence the forces contributing to RR.

Unlike the two previous terms, irrecoverable *pavement energy dissipation* is formed as a consequence of wave propagation along, across and inside the road structure that leads to an asymmetrical deflection bowl under the tyre. According to recent numerical predictions [4], stiffness of the uppermost pavement layer is much more influential than that of lower layers; thus, a stiffer upper pavement saves energy. In the scenario examined in [4], changing from a

flexible to a rigid pavement may reduce pavement RR by approximately 3 N per HGV tyre at 40 kN. Other models (e.g. Akbarian [6]) have been developed, confirming the main findings.

Knowledge gaps and objectives

Most of the studies on aggregate indentation effects have emphasised structural vibration, noise radiation, wear resistance and friction [7, 8]. Meanwhile the majority of semi-empirical, analytical and numerical models have focused on macro-distortional RR, ignoring road irregularities and associated small interfacial deformations [9, 10, 11]. Some have developed tread-asperity indentation models studying contact stress distribution, but have omitted energy loss calculations [12, 13]. Only a few have produced estimates of energy losses due to stone indentation [14, 15, 16, 17, 18], and not all of these have clearly distinguished micro-distortional loss from tyre macro-distortional loss.

Due to the lack of detailed numerical RR predictions, pavement-tyre interaction, which is believed to account for 7% - 18% of total vehicle energy consumption in Europe [8, 19], is still very much of interest. Specifically, the key factor that has been ignored is the individual stone effect (micro-distortion) with both tread inertia and visco-elastic components. None of the existing models has attempted to examine these individual components, often representing protrusions as a series of 2-D/3-D linear or non-linear spring-dampers or through spectral representation derived from scanned real-life surfaces. There is a need to fill this knowledge gap and propose an approach that would, in the long-term, assist in optimising tyre treads and road surface topography for minimal RR without compromising skid resistance and drainage function.

The objective here is to present a computationally efficient numerical multi-scale methodology in order to compute the micro-distortional RR induced by single particles of macro-texture (0.5mm – 50 mm bandwidth). The model involves macro-scale (whole tyre)

and micro-scale (tread-asperity interaction) analyses as explained below and has been developed using Abaqus commercial software.

Macro-Scale Model

The macro-scale model is of a 175 SR14 3-D slick radial Yokohama tyre adapted from Abaqus open source [25]. In accordance with the ABAQUS documentation, the first step is to generate a half axi-symmetric model for 2-D inflation analysis. The adapted tyre cross-section consists of rubber-based components such as the tread and sidewalls, and two belts and the carcass, which are made up of fiber-reinforced composites. The tread and sidewalls have been discretised with CGAX4H and CGAX3H hybrid elements with twist and modelled as a viscoelastic material, the properties of which have been supplied from the tyre manufacture. The application of this material model to a tyre construction, in which it is not actually used, is considered to be justifiable since the micro-distortional RR methodology is being proposed in generic.

In turn, the belt and carcass fiber parts have been represented as a linear elastic material with elastic modulus, Poisson's ratio and density, respectively, being equal to 172.2 GPa, 0.3, 5900 kg/m^3 and 9.87 GPa, 0.3, 1500 kg/m^3 [25]. The reinforcement belts and carcass have been meshed with a rebar layer in SFMGAX1 surface elements being embedded in host continuum elements CGAX4H. In order to prevent an offset of the embedded element nodes from the host element edges resulting from numerical roundoff, a roundoff tolerance is specified. The introduction of a roundoff technique enhances the performance by adjusting the positions of embedded elements to lie precisely on the host elements and thus minimizes the number of constraint equations used to embed surface elements.

A half 3-D tyre is produced by revolving the half cross section model about the rotation axis and then reflecting it to generate a full 3-D tyre. The analysis comprises three stages: static, braking/traction and steady-state rolling are conducted sequentially. The results from each

analysis are transferred to the subsequent models using a transfer capability. The static tyre analysis provides the boundary conditions for the braking/traction analysis, and the braking/traction model is the basis of the steady-state tyre rolling simulation. The main purpose of the macro-scale tyre model for this research is to provide loading, stationary and unloading rates for input into the micro-scale simulation.

Evaluation of tyre distortion has been carried out applying Abaqus/Standard *Steady-State Transport Analysis* in a mixed Arbitrary Lagrangian Eulerian (ALE) formulation travelling against a smooth rigid road. In this framework, the deformation is described by a Lagrangian method whilst the rigid body rotation is characterised by an Eulerian framework. To overcome local material instability, the STABILIZATION option was used to introduce artificial viscous forces. To account for nonlinearity effects that arise due to large deformations, the NLGEOM function was activated. Inclusion of centrifugal forces into the analysis has been done using the INERTIA command. Slip tolerance value F_f has been set to 0.02 as more relaxed (larger) values generally prevent convergence. Efficient computational speed has been achieved by incorporating a finer mesh in the footprint region covering 40°of arc and a coarser mesh covering the remaining 320°, both being discretised with general linear hybrid elements (C3D8H and C3D6H) suitable for incompressible material (Figure 2). The total numbers of nodes and elements in the model were 13548 and 7255, respectively, as illustrated in Figure 2. Steady-state tyre analysis was conducted under 3300 N (P_1) loading condition at an inflation pressure of 200 kPa.

Application of free rolling conditions

As a first step, free rolling conditions have to be reached, and for this it is necessary to separately (and correctly) specify the wheel velocity (V_x) and its angular velocity (Ω_2). One of the possible techniques is to determine the effective rolling radius R_{eff} of a tyre, spinning

on a frictionless surface, based on the average tread surface horizontal velocity and then to calculate the required angular velocity for steady-state rolling:

$$\omega_{freeroll} = V_x / R_{eff} \tag{2}$$

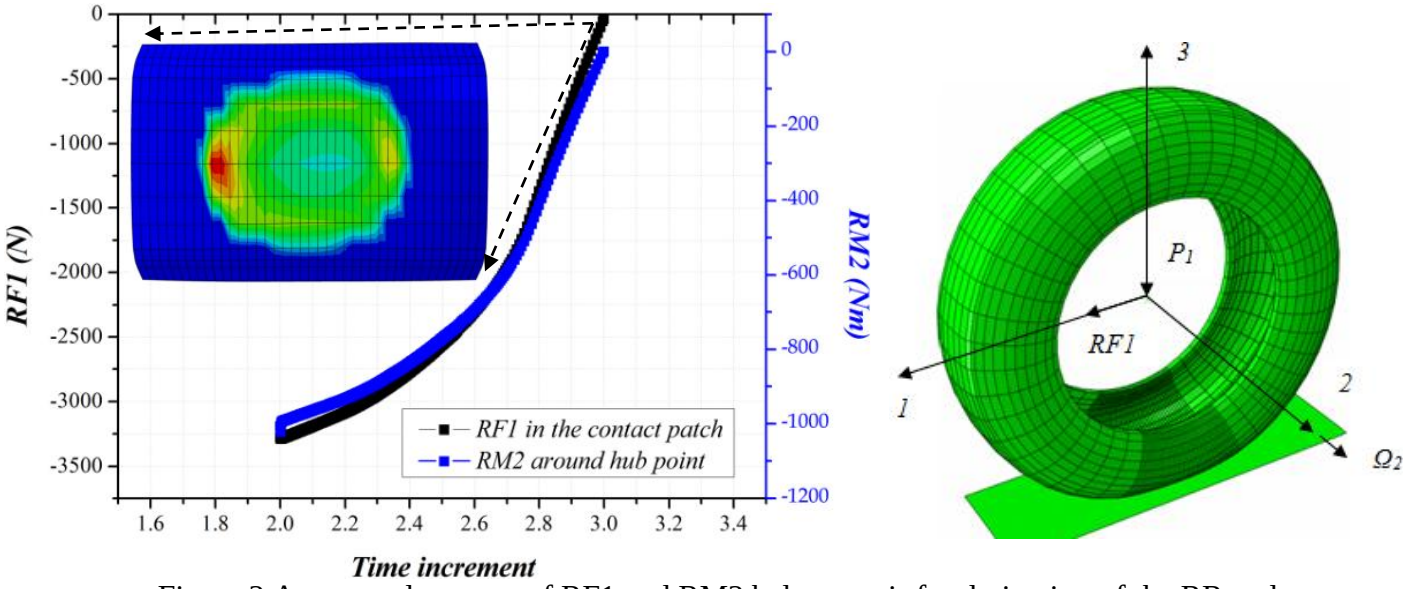

Figure 2 An example output of RF1 and RM2 balance pair for derivation of the RR and contact force distribution at the end of time step at 3300 N, 200 kPa, 0.7 coefficient of friction, 100 kph rolling speed (left) and FE-discretised tyre structure (right)

Alternatively, the free rolling angular velocity can also be found through trial and error [20] such that the moment balance about the rim centre becomes virtually zero ($\leq 0.05 Nm$, where achievable). This second approach has been applied for approximate determination of free rolling conditions. After experimentation the time step used in computation was 1.0 sec; the initial and analysis time increments were taken as 0.001 and 0.01 secs respectively. These were found to give good convergence.

The adopted procedure was as follows:

- estimate the angular velocity value for the first run
- increase/decrease the angular velocity (Ω_2) depending on RR moment about the hub

- select Ω_2 such that the RR moment (RM2 in Figure 2) ~ 0, output the reaction force in the longitudinal direction (RF1), which quantitatively equates to contact force, i.e. the *micro-distortional* RR

Despite slight numerical instability and imperfect convergence of the RR moment around the hub point, the average RR magnitudes for the Abaqus tyre matched the outcomes reported in the literature for this tyre [21].

Rubber Properties

It is well established that rubber behaviour is strongly contingent on temperature (an increase softens the compound), frequency of cyclic loading (an increase stiffens the compound) as well as strain level (an increase softens the compound) [5]. To properly apply viscoelasticity of tread compound, rheological Maxwell elements, springs and dashpots, were implemented in ABAQUS. Elastic behaviour was characterized by a reduced polynomial (Neo-Hookean) hyperelastic model applying the HYPERELASTIC command, where just one parameter was needed being expressed as a half of the shear modulus. Inclusion of the VISCOELASTIC command allowed account to be taken of the viscous contribution and this was represented by an *N*-term Prony series expansion of the dimensionless relaxation modulus in the time domain as:

$$g(t) = g_\infty + \sum_{i=1}^{N} g_i e^{(-t/\tau)}, N = 1,2,..... \quad (3)$$

where g_∞ is the long-term dimensionless modulus for the rubbery region and g_i and τ_i are material constants. Stiff and soft (higher and lower long-term modulus as compared with soft rubber) rubber compound properties were used, with 12 and 14 Prony terms respectively, corresponding to 55°C operating temperature. The modular ratio of soft to stiff rubber

amounted to 0.92. To simplify the modelling problem, strain-dependent nonlinearity (Payne and Mullins effects) was excluded from the analysis.

All tyre rubber-like parts have been assumed to have the same properties. As can be seen in Figure 3, the tyre with soft compound dissipates less energy than the stiff compound tyre.

Friction Effect

The surface friction coefficient is known to be dependent on slip velocity, pavement surface, rubber properties, temperature and contact pressure. Taking account of this, three friction models have been studied and compared, namely a simple Coulomb coefficient (equation 4), the slip-velocity-dependent coefficient (equation 5) and direct usage of test data that included contact pressure.

The parameters for the Eqn. 5 model have been extrapolated based on measurement data in Guo *et al* (2004) to match measured pressures inside the contact patch, which is a function of the inflation pressure and bulging of the tyre belt [12, 22].

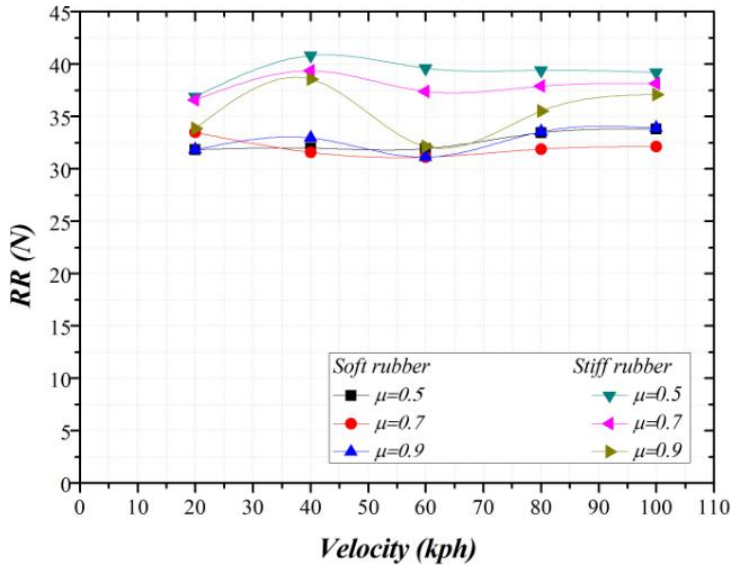

Figure 3 RR vs Velocity for Coulomb friction model for soft and stiff compound at 3300 N

$$\mu = F_{fric} / F_{ver} \tag{4}$$

$$\mu = \mu_k + (\mu_s - \mu_k)e^{-d\gamma} \tag{5}$$

where μ_k is the kinetic friction coefficient, μ_s is the static friction coefficient, d is the decay coefficient and γ is the slip velocity.

It has been determined that tyre deformation (and RR) changes only marginally when switching from a Coulomb friction model to a more complex model under free rolling conditions. For subsequent simulations, it was therefore considered reasonable to apply a constant friction coefficient. Similar results have been reported by Wang *et al* (2010).

Micro-Scale Model

A 3-D FE model utlizing the Abaqus/Explicit solver has been used to investigate contact forces between a tread block and a stone in order to deduce *micro-distortional* RR. In the first instance, Abaqus/Implicit was applied to study contact forces. However, it was abandoned due to inability to achieve a converged solution after trying various time increments, an adaptive meshing function, using a finer mesh discretisation and adaptation of contact softening/damping controls. It was therefore concluded that its applicability for this specific analysis would be difficult and computationally expensive compared to Abaqus/Explicit. The model mimics three essential tyre-pavement interaction phases: indentation of the stone into a tread compound, holding and release/snap-out. To build a simplified and efficient tread-stone interaction model, a few basic assumptions have been made:

- the tread block is a homogeneous visco-elastic rubber with no interlayer reinforcement
- surface asperities have been assumed as having an idealized hemispherical form and rigid properties (210 GPa modulus; $\nu = 0.3$) with no micro-texture
- asperity penetration takes place in the vertical direction; no tangential movement is applied

- pre-stress from macro-distortion (lateral stretching and twisting) of a tread block prior to stone-induced micro-distortion is neglected
- no adhesion forces are present
- temperature is constant

Pavement Surface Properties and Tread Pattern Assumptions

There are a wide range of asphalt mixtures all having their own surface macro-texture layout (positive/negative) and amplitude (texture depth). Aggregate gradation is a primary factor influencing road surface properties in addition to shape (angular, cubic etc) and maximum aggregate size. Overall, based on their topography, pavements could be categorised into smooth (e.g. 0/8mm Stone Mastic Asphalt) and rough (e.g. surface dressing/chip seal) types. The advantage of the model is that it allows both surface classes to be covered by considering a range of hemispherical diameters. To examine different road textures, spacing between stones can be varied along and across the contact. To simplify the problem, a hypothetical mixture is considered of a single-sized gradation making all surface stones identical. Even though the assumption of hemispherical asperities is unrealistic, it is still, as indicated by Greenwood and others [12, 24], a justifiable approximation of road chippings. In the context of RR, tyre tread designs are also important. These involve the arrangement of continuous ribs, uncoupled tread blocks, circumferential and lateral grooves as well as moulded sipes, which in part share the functions of road texture. Treads are generally classified into four groups: symmetric, asymmetric, directional and those that feature both asymmetric and directional tread patterns. It is believed that the tread pattern impacts are particularly influential for local interaction mechanics as well as tyre dynamics. Since at the micro-scale level the interaction is established between a single block and a single stone and ALE formulation does not take account of it at the macro-scale level, the tread patterns could be

implicitly incorporated via void area ratio which is the fraction of the tyre outer plane that is actually rubber (A_{rubber}) and not the profile void (A_{void}) in the contact zone.

$$VR = \frac{A_{rubber}}{A_{void} + A_{rubber}} \tag{6}$$

Boundary Conditions, Meshing, Contact Stiffness, Friction and Analysis Steps

Encastre type boundary condition (BC) has been adopted on the base of the tread block, while the surface and sides have been left free to move. The indenter (i.e. the stone) is then moved into the surface of the block. Such BCs enable consistent normal stress distribution to be obtained in comparison with a fixed stone – movable block combination, where normal stresses have been found to be inconsistent (too sensitive to contact definition).

As stated, to replicate real-life interaction, three major analysis steps have been considered, namely indentation/loading, hold/full indentation and release/unloading. In our configuration, BCs of the stone have therefore been described in terms of velocity to enable loading, holding ($V_{hold} = 0\, mm/sec$) and unloading states, which are, as summarized below, output from the macro-scale model.

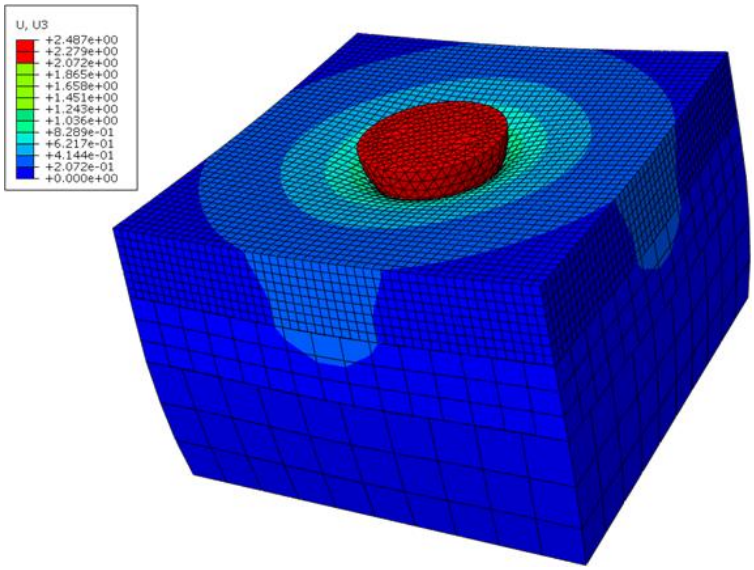

Figure 4 Illustration of a micro-scale model and mesh configuration

The block is divided into three layers: top (in contact with the stone), middle and bottom (Figure 4), with a finer mesh in the top layer surface applying 20000 8-node linear brick C3D8R elements with reduced integration and hourglass control. Due to the high rate of stone impact, distortion control is turned on**,** facilitating a more accurate computation. By varying mesh configurations, it was seen that the reducing number of elements generates a contact force distortion in the loading stage and as a result change texture-dependent RR. By optimizing the mesh, a good compromise between accuracy and computational speed was found for the selected configuration.

To reduce the number of time increments required, mass scaling is introduced. Excessive mass scaling was observed to cause substantial oscillations compared to zero mass scaling case. After checking various levels of mass scaling, an optimum factor was adopted to enable increased computational speed without generating unwanted noise.

To effectively transmit deformations of nodes through the tread-sphere interface, a contact stiffness between them needed to be established, preventing numerical overlap between contacting bodies. Having experimented with a wide range of contact stiffnesses, an optimised high, but computationally stable, level was selected for all analysis steps. Friction was assumed to be constant, but was not found to significantly affect computed forces.

Derivation of Loading and Unloading Rates for Micro-Scale Model

The indentation and release rates (Figure 5) have been extracted from the macro-scale model surface nodes as they make contact with the surface at the leading edge and leave at the trailing edge.

Figure 5 shows a vertical velocity distribution for a series of nodes before and after the velocity becomes zero in the contact area. Linear integration of vertical velocity between nodes with respect to time allowed the indentation/release velocities to be determined for specific distances from the smooth surface.

Assuming these distances correspond to indentations experienced by protruding surface texture, loading/unloading rate boundary conditions have been formulated.

It was found that similar rates applied regardless of rubber compound rigidity. The duration of the contact phase was also derived from the macro-scale data. More specifically, indentation/release durations were determined based on the length between nodes, which was constant.

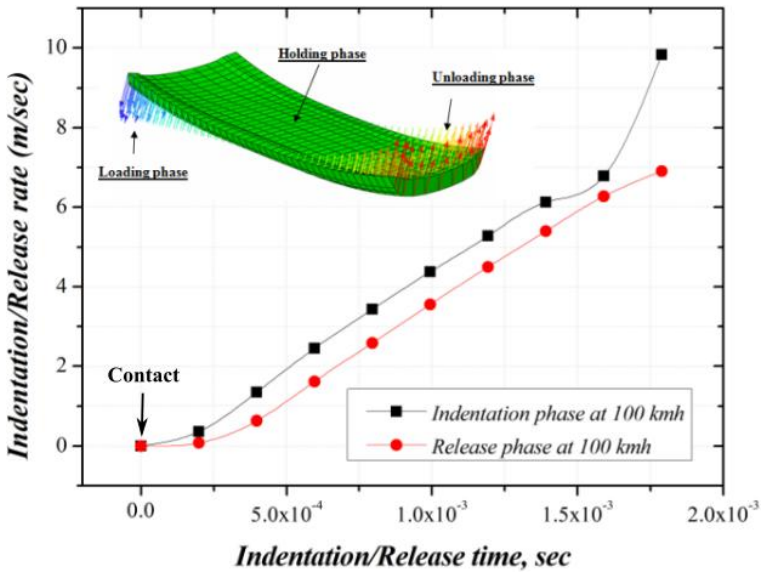

Figure 5 Vertical velocity throughout contact phases adopted from the macro-scale model

Subsequently, dividing the internode distance by a translational velocity provided time estimates. Finally, summing up all time estimates in each interval, the duration for both loading and unloading at a given indentation level was calculated. As shown in Figure 5, the indentation rates were always predicted to be higher than the release rates. This can be ascribed to rubber viscosity effects and inertia.

Micro-Distortional RR Force Estimation

The *micro-distortional* RR was derived from the moment (RRM) given by contact force distribution, as shown in Figure 6, and the number of stones in the contact at a given time. The RRM about the point on the contact patch directly below the centre of the wheel is quantified. It is then divided by the loaded tyre radius (measured in the macro-scale model) to

determine the *texture-dependent* RR for the whole tyre. An advantage of this numerical technique is that by altering stone size/shape/spacing, the influence of different texture patterns could be explored.

Results and Discussion

The computational technique described above has been applied to evaluate the compressive contact forces between a tread compound block and a hemispherical stone of 5mm radius indenting into a rubber by 0.761 mm, 0.672 mm, 0.642 mm, 0.650 mm, 0.645 mm, respectively at 20 kph, 40 kph, 60 kph, 80 kph and 100 kph. These indentation magnitudes all relate to a tyre load of 2 kN and have been found experimentally by the authors to be realistic for typical asphalt surfaces; they also agree with the order of magnitude of estimates reported in the literature [26].

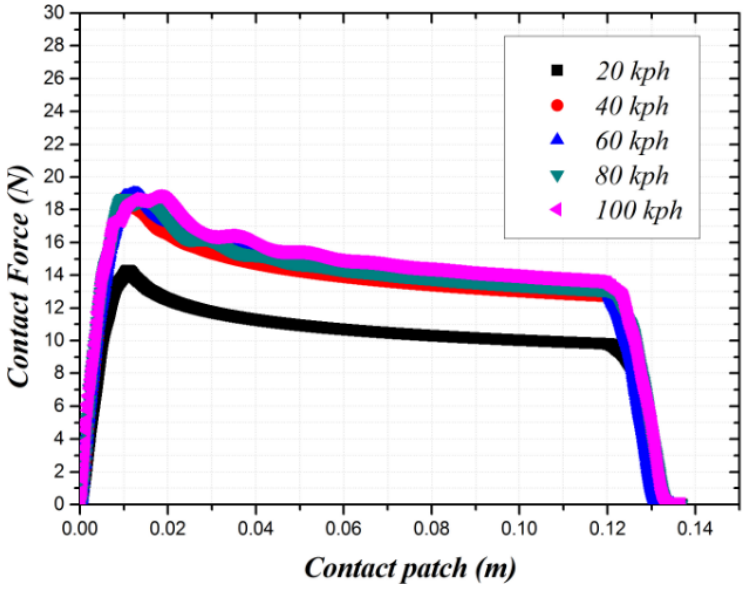

Figure 6 Typical compressive contact force distribution for a hemisphere of 5mm indenting into a tread compound by 0.5mm

As an example, the results for 0.5 mm indentation (Figure 6) clearly demonstrate that the tread-stone model captures the expected visco-elastic behavior caused by a single indenter. In particular, Figure 6 shows an asymmetrical contact force distribution: peak normal force at

the beginning of the contact region, followed by a gradual decrease of the force until the beginning of unloading phase where the indenter snaps out from the rubber surface. It can be seen that due to stiffening of the compound at higher loading rates (40, 60, 80, 100 kph), the average contact forces at these velocities are greater in magnitude by around 27% compared with 20 kph, at which speed the rubber has a longer time to relax.

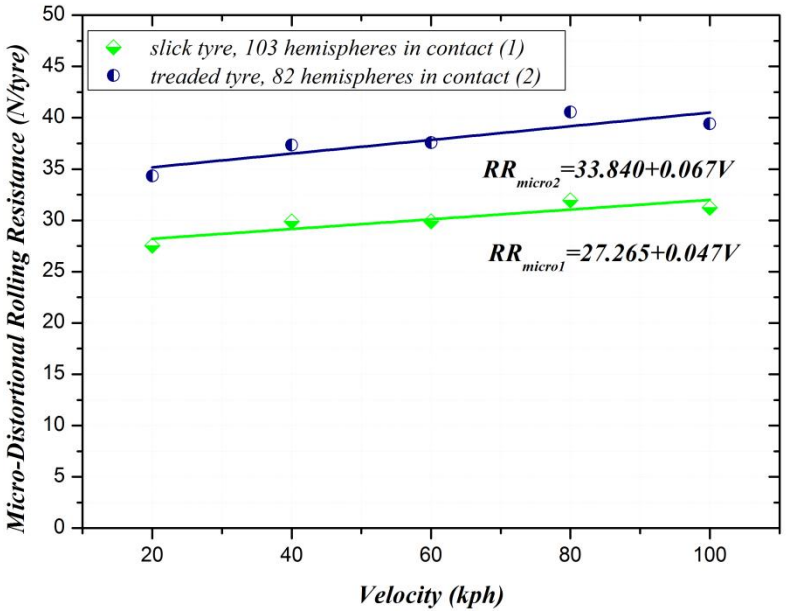

Figure 7 Micro-distortional RR for a slick and treaded tyres when, respectively, rolling over 103 and 82 hemispheres (tight packing) with 5mm radius

Examining the contact force plot, it may be noticed that the shape of the normal forces at the end of the indentation phase is distinctly different for the 20 kph case, in that no ripples are present. The ripples at higher velocities might be explained by either the stiffer tread compound at higher penetration velocities or rigid fixing of the base of the block confining the block movement and generating reflected waves. Contrary to expectations, inertia was found to impact insignificantly on compressive contact force prediction at all the loading rates used.

The example in Figure 7 illustrates the computed *micro-distortional* RR for a slick tyre, which rises linearly as velocity increases, ranging from 28 N at 20 kph to 32 N at 100 kph for

a hypothetical road surface with 103 hemispherical stones in contact with the tyre, at an average contact force of about 19.5 N/ind, represents a tyre load of about 2 kN. As can be seen the computed RR is at a similar level to the macro-distortional RR depicted in Figure 3, although this maybe rather higher than that for a real surface, due to the idealised hemispherical pavement topography (perhaps comparable to a surface dressing [15]) and the assumption that each stone indents at the centre of a tread block ignoring edge effects. The vertical projection of the wheel centre on the contact patch also carries a degree of uncertainty. The relatively small effect of velocity, this is reasonable since at a lower loading rate a slightly larger indentation would be expected due to visco-elastic effect. Taking account of tread pattern with 0.8 void ratio, typical for car tyres [27], micro-distortional RR was found to increase quite considerably. Figure 7 shows that the RR of a treaded tyre is, on average, 20 % higher than that of a slick tyre. It is expected to grow since number of contact indenters reduces to 82 (103×0.8) indenters resulting in a higher loading per stone and indentation.

A range of hemispherical radii has been examined, all with closely packed stones. At identical speeds, contact forces per indenter increase as the radius (and therefore centre-centre spacing) grows, and consequently, each indenter in the contact patch will take more force and indent deeper into the tread compound. The increase of force together with higher indentation will evidently dissipate a higher amount of energy per stone. However, when the effects are summed, a dense packing with a finer indenter will tend to induce an approximately equivalent texture-dependent RR compared to a densely packed coarser indenter.

Conclusion

A novel multi-scale approach for *micro-distortional* RR computation has been presented. It is capable of quantifying the visco-elastic response of a tread compound block indented by a

single stone. The forces, computed in the contact patch, appear to be of a reasonable distribution and magnitude, although the predicted RR is probably greater than for most real road textures. The model, though it allows useful comparison of different vehicle speeds, loads, rubber properties and texture patterns, still has to be calibrated, for real pavement surfaces by means of empirical techniques due to the hemispherical assumption.

Acknowledgements
We would like to gratefully acknowledge technical support from the staff of the Faculty of Engineering at the University of Nottingham.

References

[*1*] Ghosh, S., Sengupta, R. and Kaliske, M., "Prediction of Rolling Resistance for Truck Bus Radial Tires with Nanocomposite Based Tread Compounds Using Finite Element Simulation," *Journal of Rubber Chemistry and Technology*, Vol. 87, 2014, pp.576-590.

[*2*] Pettinari, M., Schmidt, B., Bo Jensen, B., and Hededal, O., "New surface layers with low rolling resistance tested in Denmark," *Submitted to ISAP*, Draft Version, 2014

[*3*] Sandberg, U.,"Road Macro- and Megatexture Influence on Fuel Consumption," *Surface Characteristics of Roadway: International Research and Technologies, ASTM STP 1031*, American Society for Testing and Materials, Philadelphia, 1990, pp. 460–479.

[*4*] Lu, T. "The Influence of Pavement Stiffness on Vehicle Fuel Consumption," PhD Dissertation, University of Nottingham, UK, 2010

[*5*] Societe de Technologie Michelin, "The Tyre: Rolling Resistance and Fuel Savings," Michelin, 2003

[*6*] Akbarian, M. and Ulm F-J. "Model ," *Report*, Concrete Sustainability Hub, Massachusetts Institute of Technology, Cambridge, USA

[*7*] Sridharan, K., and Sivaramakrishnan, R., "Dyamic Behaviour of Tyre Tread Block," *American Journal of Engineering and Applied Science*, Vol. 5, 2012, pp. 119-127.

[*8*] Pinnington, R., "Tyre-road contact using a particle-envelope surface model," *Journal of Sound and Vibration*, Elsevier, Vol. 332, 2013, pp. 7055-7075.

[*9*] Hall, D. E. and Moreland, J. C., "Fundamentals of Rolling Resistance," *Journal of Rubber Chemistry and Technology*, Vol. 74, 2001, pp. 525–539.

[*10*] Kroeger, M. and Moldenhauver, P., "Influences on the vibration frequencies of tire tread block", Proceedings of ISMA 2010 including USD2010, 2010, pp. 4015-4021

[*11*] van der Steen, R., "Enhanced Friction Modeling For Steady-State Rolling Tires" Ph.D. Dissertation, Eindhoven University of Technology, Eindhoven, 2010.

[*12*] Liu, S., Sutcliffe, M. P. F., and Graham, W.R., "Prediction of tread block forces for a free-rolling tyre in contact with a rough road," *Wear*, Vol. 282-283, 2012, pp. 1–11.

[*13*] Kozhevnikov, I., Duhamel, D., Yin, H., Cesbron, J., and Anfosso-Ledee, F., "A new algorithm for computing the indentation of a rigid body of arbitrary shape on a visco-elastic half-space," *International Journal of Mechanical Sciences*, Vol. 50, 2008, pp. 1194-1202.

[14] Boere, S., Arteaga, I. L., Kuijpers, A. and Nijmeijer, H., "Tyre/Road Interaction Model for the Prediction of Road Texture Influence on Rolling Resistance," *International Journal Vehicle Design*, Vol. 65, 2014, pp. 202–221.

[*15*] Hoever, C., "The Simulation of Car and Truck Tyre Vibrations, Rolling Resistance and Rolling Noise," Ph.D. Dissertation, Chalmers University of Technology, Goeteborg, 2014.

[*16*] Fraggstedt, M., "Vibrations, Damping and Power Dissipation in Car Tyres" Ph.D. Dissertation, Royal Institute of Technology, Stockholm, 2008.

[*17*] Lopez Arteaga, I., and Nijmeijer, H. "Visco-elastic Contact Model for The Prediction of Tyre/Road Contact Forces and Rolling Resistance," *18th International Congress on Sound and Vibration*, Proceedings of ICSV, Rio de Janeiro, 2011, pp. 1–8.

[*18*] Beyer, R., and Nackenhorst, U. "Thermo-mechanical rough surface contact of rubber – like solids," *11th World Congress on Computational Mechanics*, Barcelona, 2014.

[*19*] Holmberg, K., Andersson, P. and Erdermir, A., "Global Energy Consumption due to Friction in Passanger Cars," *Tribology International*, Vol. 47, 2012, pp. 221–234.

[*20*] Wang, H., Al-Qadi, I., Stanciulescu, I. "Effect of Friction on Rolling Tire – Pavement Interaction," *Final Report, NEXTRANS Project,* No.049IY02, 2010.

[*21*] Behnke, R., and Kaliske, M. "Computation of Energy Dissipation in Visco-Elastic Materials at Finite Deformation," *Proceedings of Applied Math. Mech.*, Vol. 13, 2013, pp. 159-160.

[*22*] Guo, K., Zhuang, Y., Chen, S. and William, L. "Experimental Research on Friction of Vehicle Tire Rubber," *Chinese Journal of Mechanical Engineering*, Vol. 40, 10, 2004.

[*23*] Rhyne, T., and Cron, S. "A study on Minimum Rolling Resistance," *Tire Science and Technology*, TSTCA, Vol. 40, 4, 2012, pp. 220-233.

[*24*] Greenwood, J. and Wu, J. "Surface Roughness and Contact: An Apology", *Meccanica*, 36, 2001, pp. 617-630.

[*25*] ABAQUS (2014) "ABAQUS Documentation", Dassault Systèmes, Providence, RI, USA.

[*26*] "Integrated Tire and Road Interaction – Development of a Tire-Road Friction Model", *Specific Targeted Research or Innovation Project*, FP6-PL-0506437, Deliverable 5.1, 2006.

[*27*] Walter, J. "Tire Construction and Materials", *Tyre-Vehicle Dynamics Online Course*, University of Akron, 2015

List of Figure Captions

FIG. 1 — *Close-up view of multi-indentation effects as a result of array of stones (not to scale)*